Electronic Supplementary Information

A highly Mn^{2+}-doped narrowband green phosphor toward wide color-gamut display applications

Chenyang Zhan[a,b,c,d], Haomiao Zhu,[a,b,c,d] Sisi Liang,[c,d] Yingping Huang,[c,d] Zihao Wang,[c,d] and Maochun Hong*[a,b,c,d]*

a. School of Rare Earths, University of Science and Technology of China, Hefei, Anhui 230026, China

b. Ganjiang Innovation Academy, Chinese Academy of Sciences, Ganzhou, Jiangxi 341119, China

c. Fujian Science & Technology Innovation Laboratory for Optoelectronic Information of China, Fuzhou, Fujian 350108, China

d. Xiamen Key Laboratory of Rare Earth Photoelectric Functional Materials, Xiamen Research Center of Rare Earth Materials, Haixi Institute, Chinese Academy of Sciences, Xiamen 361021, China

E-mail: zhm@fjirsm.ac.cn

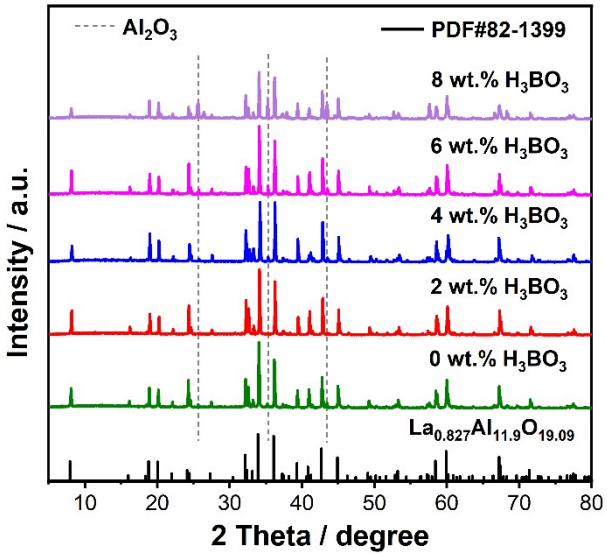

Fig. S1 XRD patterns of the LAO:0.30Mn^{2+} samples synthesized with the addition of various amounts of H_3BO_3 as flux.

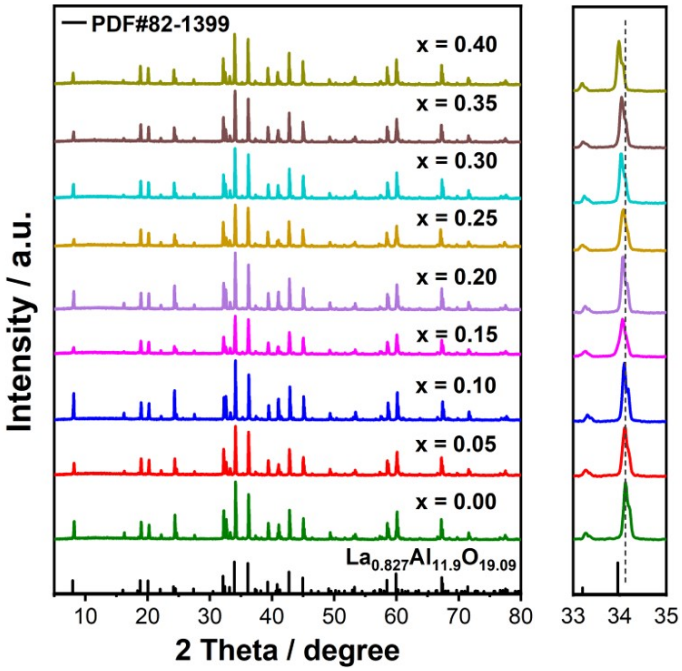

Fig. S2 XRD patterns of the LAO:*x*Mn^{2+} (x = 0.00 – 0.40) samples synthesized with the addition of 2 wt.% H_3BO_3 as flux.

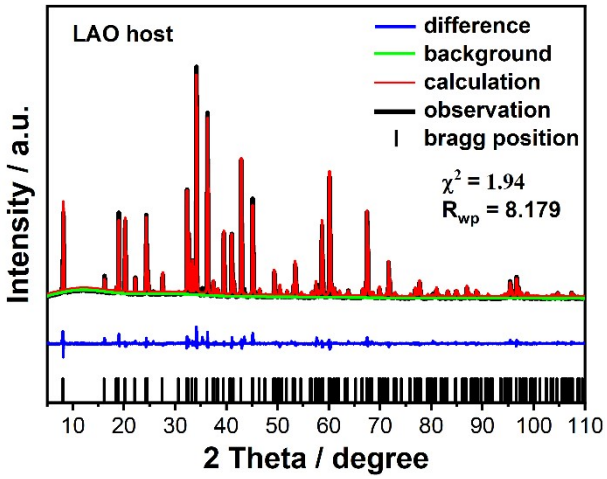

Fig. S3 Rietveld refinement on the XRD pattern of the undoped LAO sample.

Table S1. The obtained crystallographic data for the undoped LAO and LAO:0.30Mn^{2+} samples based on Rietveld refinement.

Formula	LAO	LAO:0.30Mn^{2+}
Crystal system	hexagonal	hexagonal
Space group	P63/mmc	P63/mmc
a = b (Å)	5.56162	5.57311
c (Å)	22.04610	22.10693
α = β (°)	90	90
γ (°)	120	120
V ($Å^3$)	590.562	592.681
R_{wp} (%)	8.179	6.338
χ^2	1.94	1.34

Table S2. Atomic coordinates of the undoped LAO sample based on XRD Rietveld refinement.

Atom	x	y	z	frac	U_{iso}
La(1)	0.6667	0.3333	0.2500	0.4900	0.0155
La(2)	0.7161	0.4321	0.2500	0.1150	0.0033
Al(1)	0.8308	0.6616	0.1069	0.9200	0.0100
Al(2)	0.3333	0.6667	0.0269	1.0000	0.0199
Al(3)	0.3333	0.6667	0.1901	1.0000	0.0142
Al(4)	0.0000	0.0000	0.0000	1.0000	0.0188
Al(5)	0.0000	0.0000	0.2394	0.4250	0.0230
Al(6)	1.0097	1.0194	0.2087	0.0480	0.2096
O(1)	0.1554	0.3108	0.0521	1.0000	0.0120
O(2)	0.5036	0.0072	0.1453	1.0000	0.0196
O(3)	0.6667	0.3333	0.0546	1.0000	0.0164
O(4)	0.0000	0.0000	0.1446	1.0000	0.0242
O(5)	0.1861	0.3712	0.2500	1.0000	0.0356

Table S3. Atomic coordinates of LAO:0.30Mn^{2+} based on XRD Rietveld refinement.

Atom	x	y	z	frac	U_{iso}
La(1)	0.6667	0.3333	0.2500	0.4900	0.0017
La(2)	0.7094	0.4188	0.2500	0.1150	0.0039
Al(1)	0.8292	0.6583	0.1075	0.9200	0.0056
Al(2)	0.3333	0.6667	0.0305	0.7000	0.0173
Al(3)	0.3333	0.6667	0.1903	1.0000	0.0046
Al(4)	0.0000	0.0000	0.0000	1.0000	0.0090
Al(5)	0.0000	0.0000	0.2376	0.4250	0.0008
Al(6)	0.8436	0.6872	0.1080	0.0480	0.0034
O(1)	0.1529	0.3058	0.0526	1.0000	0.0069
O(2)	0.5044	0.0088	0.1484	1.0000	0.0119
O(3)	0.6667	0.3333	0.0564	1.0000	0.0149
O(4)	0.0000	0.0000	0.1486	1.0000	0.0126
O(5)	0.1768	0.3537	0.2500	1.0000	0.0289
Mn	0.3333	0.6667	0.0305	0.3000	0.0173

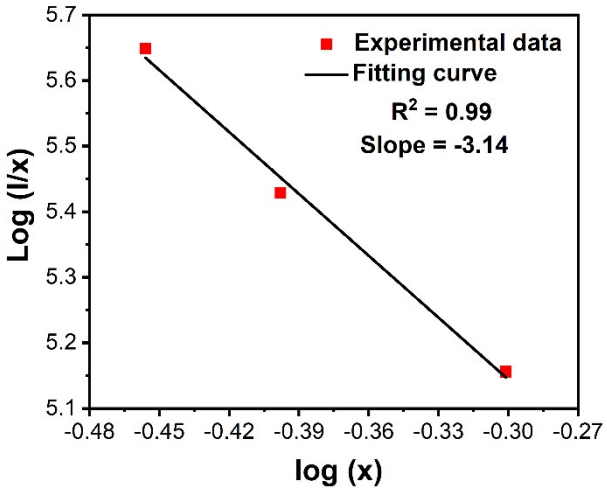

Fig. S4 The relationship between log(*x*) and log(*I*/*x*) in LAO:*x*Mn^{2+} (*x* = 0.35, 0.40, 0.50) samples.

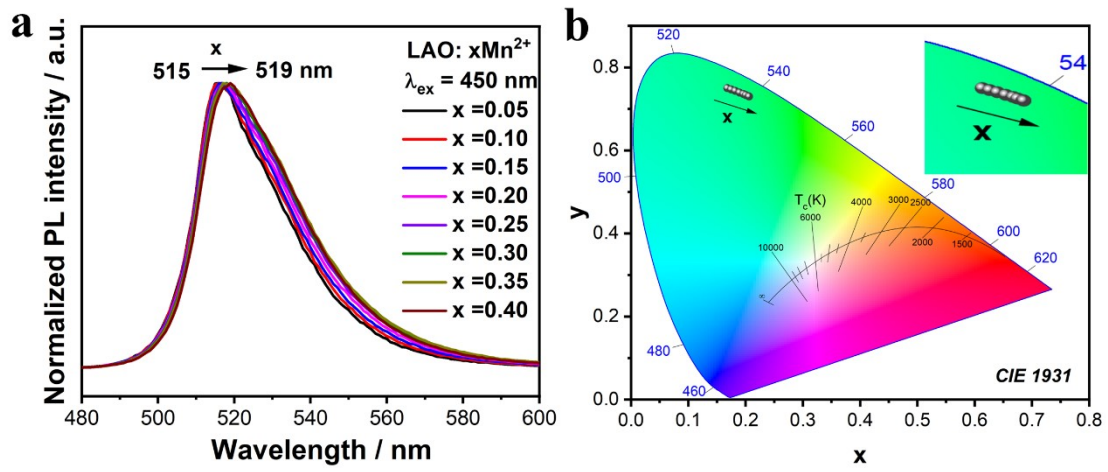

Fig. S5 a) The normalized PL spectra of the LAO:xMn^{2+} samples. b) CIE 1931 chromaticity coordinates of the LAO:xMn^{2+} (x = 0.05 – 0.40) samples.

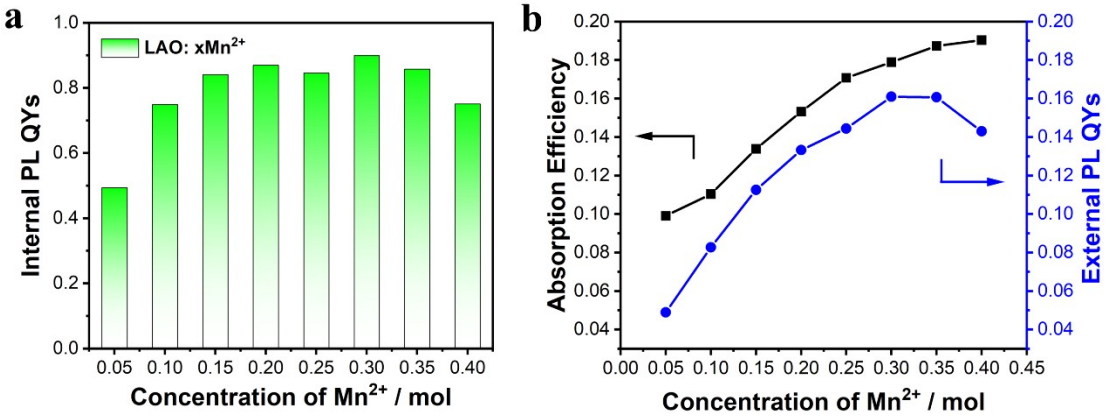

Fig. S6 a) The measured internal PL QYs of the LAO:xMn^{2+} (x = 0.05 – 0.40) samples under excitation at 450 nm. b) The absorption efficiency and external PL QYs as a function of Mn^{2+} doping concentration.

Table S4. The internal PL QYs, absorption efficiency, and external PLQYs of the

LAO:xMn^{2+} (x = 0.05 – 0.40) samples.

x(mol)	Internal PL QYs	Absorption efficiency	External PL QYs
0.05	0.4938	0.0990	0.0489
0.10	0.7487	0.1104	0.0826
0.15	0.8407	0.1338	0.1125
0.20	0.8693	0.1533	0.1332
0.25	0.8458	0.1707	0.1444
0.30	0.8997	0.1789	0.1610
0.35	0.8576	0.1873	0.1607
0.40	0.7509	0.1903	0.1429

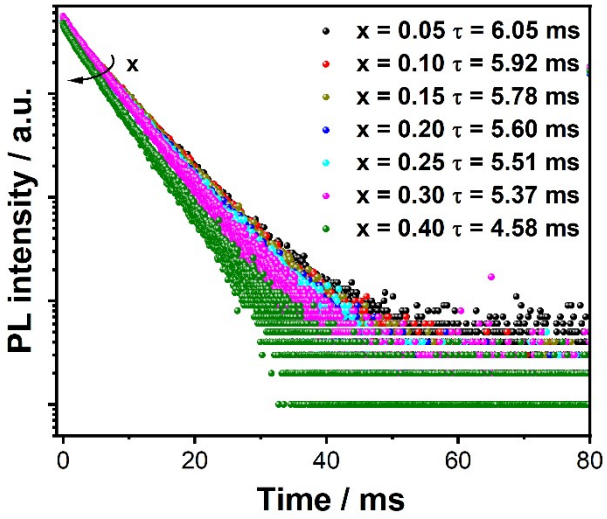

Fig. S7 The PL decay curves of the LAO:xMn^{2+} (x = 0.05 – 0.40) samples by monitoring emission at 517 nm under excitation at 450 nm.

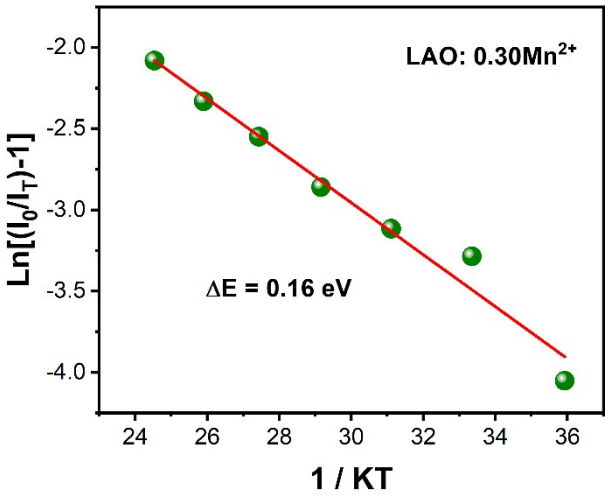

Fig. S8 The Arrhenius plot of the temperature dependence of the integrated emission intensity of the LAO:0.30Mn^{2+} sample.

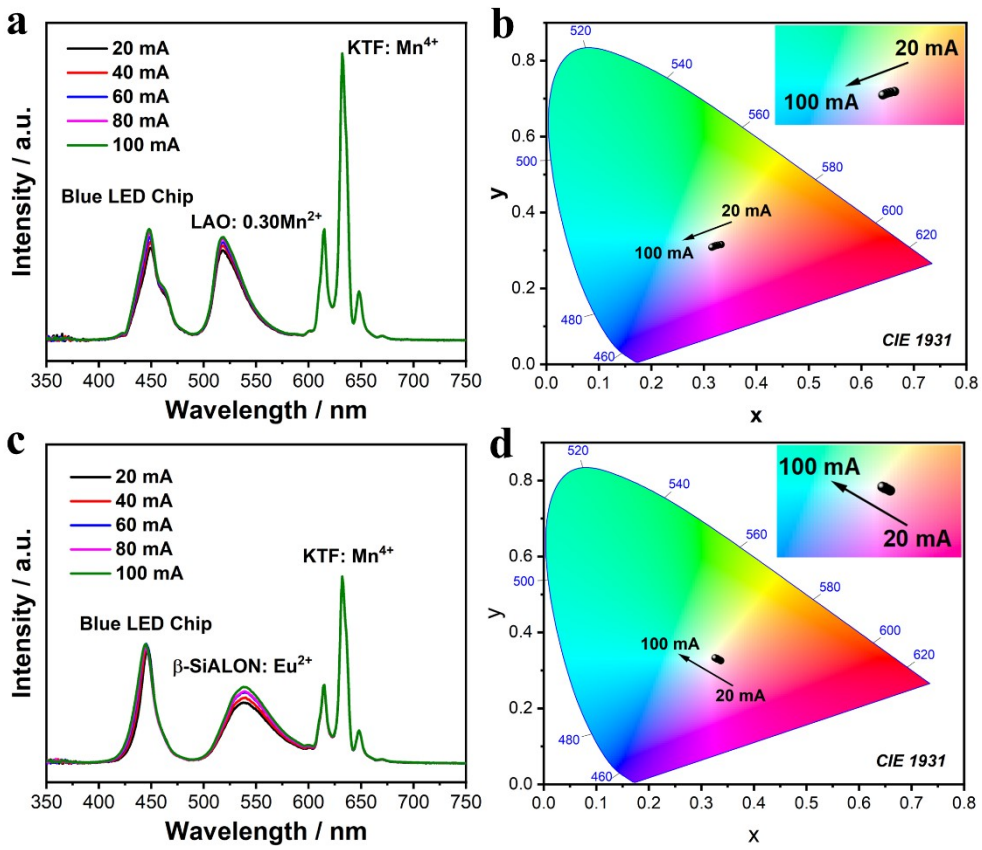

Fig. S9 The a) electroluminescence (EL) spectra and b) CIE 1931 chromaticity coordinates of LED1 under various drive currents (20 – 100 mA). The c) EL spectra and d) CIE 1931 chromaticity coordinates of LED2 under various drive currents (20 – 100 mA).

Table S5. The comparison of several green phosphors.

Phosphors	Peak (nm)	FWHM (nm)	Thermal stability	Internal/ external PL QYs	CG[a)] (NTSC)	CCT (K)	Ref
β-SiALON:Eu^{2+}	540	54	81%/473 K	97%/71%	96%	8379	1
$Ba[Li_2(Al_2Si_2)N_6]:Eu^{2+}$	532	57	70%/473 K	–/–	–	–	2
$RbLi(Li_3SiO_4)_2:Eu^{2+}$	530	42	103%/423 K	80%/29%	107%	6221	3
$RbNa(Li_3SiO_4)_2:Eu^{2+}$	523	41	102%/425 K	96%/42%	113%	5196	4
$Sr_2Li(Al, Ga)O_4:Eu^{2+}$	512	40	60%/423 K	42%/–	107%	10740	5
γ-AlON:Mn^{2+}, Mg^{2+}	520	44	76%/473 K	62%/–	102.4%	10611	6
$MgAl_2O_4:Mn^{2+}$	525	36	107%/473 K	45%/–	116%	10342	7
$Sr_2MgAl_{22}O_{36}:Mn^{2+}$	518	26	82%/473 K	75%/42%	127%	–	8
$BaZnAl_{10}O_{17}:Mn^{2+}$	516	31	90%/473 K	86%/26%	110%	7804	9
$Ba_{0.75}Al_{11}O_{17.25}:Mn^{2+}$	512	28	–	–/–	107.3%	6645	10
$Zn_4B_6O_{13}:Mn^{2+}$	540	33	98%/523K	72%/–	75%	3960	11
$La_{0.827}Al_{11.9}O_{19.09}:Mn^{2+}$	517	28	89%/473 K	90%/16%	124%	5464	TW[b)]

[a)] CG represents color gamut.

[b)] TW represents this work.

Reference

1. S. Li, L. Wang, D. Tang, Y. Cho, X. Liu, X. Zhou, L. Lu, L. Zhang, T. Takeda, N. Hirosaki and R.-J. Xie, Achieving High Quantum Efficiency Narrow-Band β-Sialon:Eu^{2+} Phosphors for High-Brightness LCD Backlights by Reducing the Eu^{3+} Luminescence Killer, *Chem. Mater.*, 2017, **30**, 494-505.
2. P. Strobel, S. Schmiechen, M. Siegert, A. Tücks, P. J. Schmidt and W. Schnick, Narrow-Band Green Emitting Nitridolithoalumosilicate $Ba[Li_2(Al_2Si_2)N_6]:Eu^{2+}$ with Framework Topology whj for LED/LCD-Backlighting Applications, *Chem. Mater.*, 2015, **27**, 6109-6115.
3. M. Zhao, H. Liao, L. Ning, Q. Zhang, Q. Liu and Z. Xia, Next-Generation Narrow-Band Green-Emitting RbLi(Li(3)SiO(4))(2):Eu(2+) Phosphor for Backlight Display Application, *Adv. Mater.*, 2018, **30**, 1802489.
4. H. Liao, M. Zhao, Y. Zhou, M. S. Molokeev, Q. Liu, Q. Zhang and Z. Xia, Polyhedron Transformation toward Stable Narrow-Band Green Phosphors for

Wide-Color-Gamut Liquid Crystal Display, *Adv. Fct. Mater.*, 2019, **29**, 1901988.

5. J. Qiao, Y. Zhou, M. S. Molokeev, Q. Zhang and Z. Xia, Narrow Bandwidth Luminescence in $Sr_2Li(Al, Ga)O_4:Eu^{2+}$ by Selective Site Occupancy Engineering for High Definition Displays, *Laser Photonics Rev.*, 2021, **15**, 2100392.
6. Q. Dong, F. Yang, J. Cui, Y. Tian, S. Liu, F. Du, J. Peng and X. Ye, Enhanced narrow green emission and thermal stability in γ-AlON:Mn^{2+}, Mg^{2+} phosphor via charge compensation, *Ceram. Int.*, 2019, **45**, 11868-11875.
7. E. H. Song, Y. Y. Zhou, Y. Wei, X. X. Han, Z. R. Tao, R. L. Qiu, Z. G. Xia and Q. Y. Zhang, A thermally stable narrow-band green-emitting phosphor $MgAl_2O_4:Mn^{2+}$ for wide color gamut backlight display application, *J. Mater. Chem. C*, 2019, **7**, 8192-8198.
8. Y. Zhu, Y. Liang, S. Liu, H. Li and J. Chen, Narrow-Band Green-Emitting $Sr_2MgAl_{22}O_{36}:Mn^{2+}$ Phosphors with Superior Thermal Stability and Wide Color Gamut for Backlighting Display Applications, *Adv. Opt. Mater.*, 2019, **7,** 1801419.
9. H. Li, Y. Liang, S. Liu, W. Zhang, Y. Bi, Y. Gong and W. Lei, Highly Efficient Green-Emitting Phosphor $BaZnAl_{10}O_{17}:Mn^{2+}$ with Ultra-Narrow Band and Extremely Low Thermal Quenching for Wide Color Gamut LCD Backlights, *Adv. Opt. Mater.*, 2021, **9,** 2100799.
10. J. Hu, E. Song, Y. Zhou, S. Zhang, S. Ye, Z. Xia and Q. Zhang, Non-stoichiometric defect-controlled reduction toward mixed-valence Mn-doped hexaaluminates and their optical applications, *J. Mater. Chem. C*, 2019, **7**, 5716-5723.
11. W. Wang, H. Yang, M. Fu, X. Zhang, M. Guan, Y. Wei, C. C. Lin and G. Li, Superior thermally-stable narrow-band green emitter from Mn^{2+}-doped zero thermal expansion (ZTE) material, *Chem. Eng. J.*, 2021, **415**, 128979.